[13] $K_2[Cr_3O(OOCH)_6(H_2O)_{2.5}(CH_3OH)_{0.5}]_2[\alpha\text{-}SiW_{12}O_{40}]\cdot 8\,CH_3OH$ was crystallized from a methanol solution of **2**. Crystallographic data for $K_2[Cr_3O(OOCH)_6(H_2O)_{2.5}(CH_3OH)_{0.5}]_2[\alpha\text{-}SiW_{12}O_{40}]\cdot 8\,CH_3OH$: orthorhombic $Pna2_1$, $a = 24.796(6)$, $b = 15.406(3)$, $c = 22.042(5)$ Å, $Z = 4$, $R_1 = 0.0480$; $wR2 = 0.0480$.

[14] D. Li, K. Kaneko, *Chem. Phys. Lett.* **2001**, *335*, 50.

[15] In the crystal structure of $K_2[Cr_3O(OOCH)_6(H_2O)_{2.5}(CH_3OH)_{0.5}]_2$-$[\alpha\text{-}SiW_{12}O_{40}]\cdot 8\,CH_3OH$, methanol molecules are hydrogen bonded to the oxygen atoms of the bridging units of the macro cations.

[16] The amount of methanol absorbed in Figure 5 seemed to be different from that in Figure 3a. This can be explained by the different equilibrium in the liquid–solid phase from that in the gas–solid phase.

A Self-Assembled Porphyrin Box from *meso*–*meso*-Linked Bis{5-*p*-pyridyl-15-(3,5-di-octyloxyphenyl)porphyrinato zinc(II)}**

Akihiko Tsuda, Takeshi Nakamura, Shigeru Sakamoto, Kentaro Yamaguchi, and Atsuhiro Osuka*

Well-ordered architectures of self-assembling porphyrins[1] have been attracting considerable interest in light of potential applications in material science,[2] template-directed synthesis,[3] reaction catalysis,[4] and duplication of photosynthetic functions of light harvesting and charge separation.[5] Among these, the coordination interaction between zinc porphyrin and pyridine groups have been often used to construct self-assembled porphyrin architectures both in infinite and discrete forms.[1–6] Fleischer and Shachter have reported a linear infinite polymeric aggregate from 5-*p*-pyridyl-10,15,20-triphenylporphyrinato zinc(II),[6] whereas Hunter and co-workers reported the formation of a cyclic tetramer from a zinc(II) porphyrin bearing a *p*-(isonicotinamide)phenyl group[7] and Imamura and co-workers reported a similar cyclic tetramer from 5-*p*-pyridyl-10,15,20-triaryl porphyrinato ruthenium(II),[8] both without X-ray crystal structures. Herein, we report a self-assembling cyclic tetramer of 5-*p*-pyridyl-15-(3,5-di-*tert*-butylphenyl)porphyrinato zinc(II) (**Z1**) with its X-ray structure and a self-assembling box-shape tetramer of *meso*–*meso*-linked bis{5-*p*-pyridyl-15-(3,5-di-octyloxyphenyl)porphyrinato zinc(II)} (**Z2**; Scheme 1). In the latter case, a very stable supramoleuclar aggregate is constructed as a result of many cooperative interactions with simultaneous structural rigidification, as suggested by its unique absorption and fluorescence spectra.

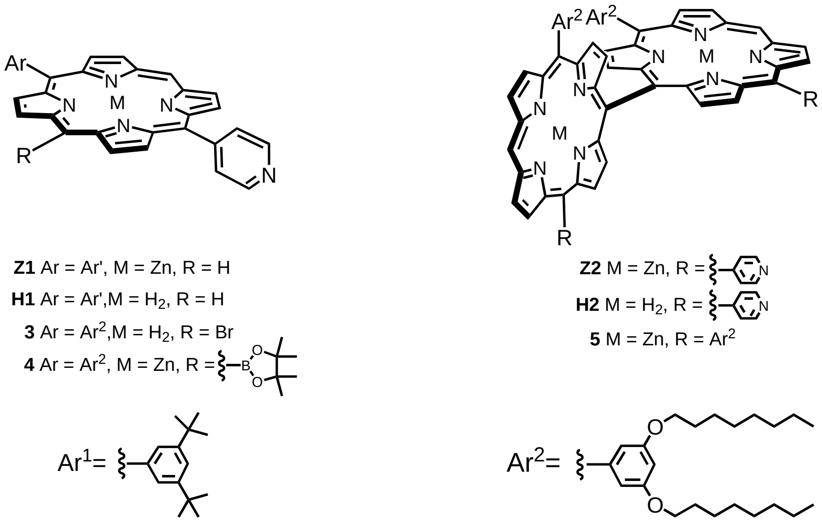

Scheme 1.

5-*p*-Pyridyl-15-(3,5-di-*tert*-butylphenyl)porphyrin (**H1**) was prepared by condensation of 4-pyridinecarboxaldehyde and 3,5-di-*tert*-butylbenzaldehyde with 2,2′-dipyrrylmethane in 8% yield, and subsequent zinc insertion with $Zn(OAc)_2$ afforded **Z1** quantitatively. The ^1H NMR spectrum of **Z1** in $CDCl_3$ is concentration independent at >3 mM and exhibits large upfield shifts for the pyridyl protons at $\delta = 6.18$ and 2.17 ppm in comparison to those of **H1** at $\delta = 8.29$ and 7.81 ppm, which indicates the coordination of the pyridyl group to zinc(II) porphyrin. As judged from the chemical shifts of the pyridyl group, **Z1** forms a similar aggregate in C_6D_6 ($\delta = 5.94$ and 2.59 ppm) but exists in a monomeric form in $[D_8]$THF ($\delta = 8.97$ and 8.31 ppm). The latter result suggested the coordination of THF to the zinc center, thus preventing self-assembling. Vapor pressure osmometry (VPO) in $CHCl_3$ afforded average molecular weights of $2760 \pm 370\,g\,mol^{-1}$ for **Z1** and $550 \pm 20\,g\,mol^{-1}$ for **H1** in a range of $3.0–13.0 \times 10^{-3}$ M, which correspond to $(\mathbf{Z1})_4$ and monomeric **H1**, respectively. The absorption spectrum of **Z1** in $CHCl_3$ is concentration dependent in an range of roughly 10^{-6}–10^{-5} M and shows the Q-band at 540 nm at $<10^{-6}$ M and at 549 nm at $>$ about 10^{-5} M (Figure 1), which correspond, respectively, to four-coordinate and five-coordinate zinc porphyrin units. A good fit for the observed sigmoidal curve is obtained by assuming porphyrin tetramer formation ($(\mathbf{Z1})_4$), which gives an association constant of $K_4 = 1.4 \times 10^{15}\,M^{-3}$.[9]

---

[*] Prof. A. Osuka, Dr. A. Tsuda, T. Nakamura
Department of Chemistry
Graduate School of Science
Kyoto University
Sakyo-ku, Kyoto 606-8502 (Japan)
Fax: (+81) 75-753-3970
E-mail: osuka@kuchem.kyoto-u.ac.jp

Dr. S. Sakamoto, Prof. K. Yamaguchi
Chemical Analysis Center
Chiba University
Yayoi-cho, Inage-ku, Chiba 263-8522 (Japan)

[**] This work was supported by Grant-in-Aids for Scientific Research from the Ministry of Education, Science, Sports and Culture of Japan and CREST (Core Research for Evolutional Science and Technology) of the Japan Science and Technology Corporation (JST). A.O. thanks the Toray Science Foundation. A.T. thanks the JSPS (Japan Society for the Promotion of Science) Research Fellowship for Young Scientists.

Supporting information for this article is available on the WWW under http://www.angewandte.org or from the author.

1433-7851/02/4115-2817 $ 20.00+.50/0

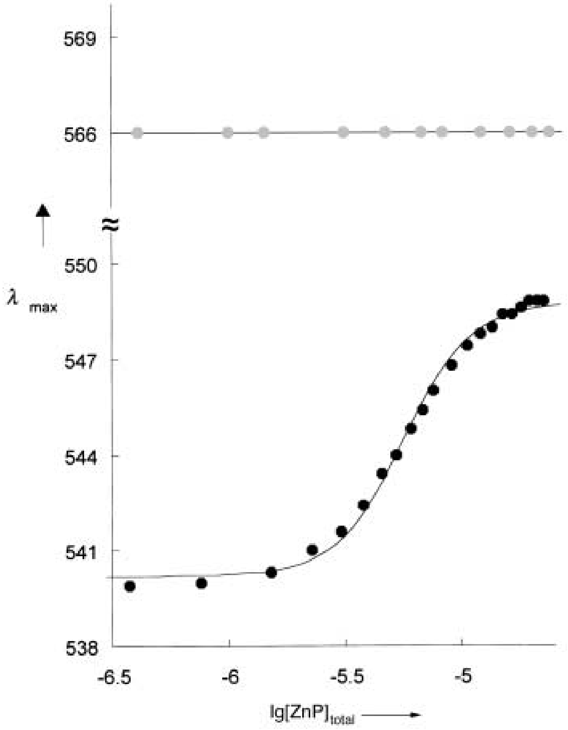

Figure 1. Concentration dependences (3.8×10^{-7}–2.3×10^{-5} M) of Q-bands of **Z1** (●) and **Z2** (●) in $CHCl_3$ at 25 °C. Solid line for **Z1** is the theoretical curve obtained by curve-fitting analysis for tetramer formation with $K_4 = 1.4 \times 10^{15}$ M^{-3}.

Slow diffusion of CH_3CN vapor into THF and benzene solutions of **Z1** gave two types of single crystals, which were both suitable for X-ray crystallography. In the crystal obtained from THF solution, **Z1** molecules coordinated by two THF molecules are arranged in a parallel manner without noticeable inter-porphyrin interaction (see Supporting Information), while in the crystal obtained from benzene solution, four **Z1** molecules form a square structure by the complementary coordination of the pyridyl groups to the zinc center (Figure 2).[10] In this structure, the Zn–N bond lengths are 2.18 Å and 2.17 Å and the central zinc units displaced out of the porphyrin plane ($C_{20}N_4$) toward the axial pyridyl group by 0.44 and 0.42 Å. The dihedral angles between porphyrin mean planes are 89.1°and 90.9°. Both of the crystal structures are consistent with the behavior of the compounds in solution.

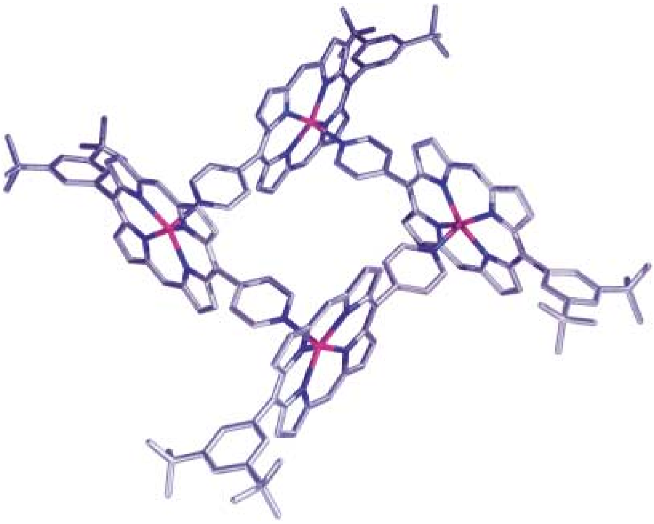

Figure 2. Molecular structure of self-assembled (**Z1**)$_4$ crystallized from benzene and CH_3CN. Hydrogen atoms and incorporated benzene molecules are omitted for clarity.

We examined the self-assembling behavior of *meso–meso*-linked zinc(II) diporphyrin **Z2** which has a unique perpendicular conformation. The silver(I)-promoted coupling reaction of **Z1** did not provide **Z2**, probably because of the presence of *meso*-pyridyl group.[11] Instead, free-base diporphyrin **H2** (Scheme 1) was prepared by Suzuki-coupling[12] of bromide **3** and boronic ester **4** in 40 % yield, and was converted into (**Z2**)$_4$ quantitatively. The sharp resonanance peaks in the ^{1}H NMR spectrum of (**Z2**)$_4$ in $CDCl_3$ excludes the formation of infinite polymeric aggregates (Figure 3). The pyridyl protons appear as split signals at $\delta = 6.59$ and 6.34 ppm, and $\delta = 2.88$ and 2.38 ppm, being shifted considerably upfield compared with those of **H2** at $\delta = 8.97$ and 8.19 ppm. Similarly the *ortho* protons in the 3,5-di-octyloxyphenyl group appear as split signals at $\delta = 7.32$ and 7.30 ppm, and the signals of the two octyloxy groups appear at different chemical shifts. These ^{1}H NMR data strongly suggest the formation of a self-assembled box-shape cyclic tetramer from **Z2** (Scheme 2, path a). A stable (**Z2**)$_4$ aggregate was inferred from the gel-permeation chromatography (GPC) HPLC with $CHCl_3$ as an eluent. Whereas the retention times of **H1** (18.4 min) and **Z1** (19.3 min) were found to be nearly the same, which suggests the dissociation of (**Z1**)$_4$ under the eluting dilute conditions, (**Z2**)$_4$ exhibited a sharp elution band with a distinctly shorter retention time (13.9 min) than that of **H2** (16.3 min), suggesting the preservation of the discrete (**Z2**)$_4$ aggregate. In THF, cold spray ionization mass spectrometry (CSI-MS)[13] detected the parent ion of (**Z2**)$_4$ at 6258, which is exactly the position expected for (**Z2**)$_4$ (calcd M_r for $C_{376}H_{400}N_{40}O_{16}Zn_8 = 6258$; Figure 4). It is notable that an intense peak assigned to (**Z2**)$_4$ was practically the sole signal and peaks attributable to smaller fragments of monomer and dimer were scarcely detected, again suggesting a stable (**Z2**)$_4$ aggregate in solution.

The absorption spectrum of (**Z2**)$_4$ in $CHCl_3$ characteristically exhibits a split Soret band ($\lambda_{max} = 426$ and 433 nm) the splitting width of which is much less than that of the normal *meso–meso*-linked zinc(II) diporphyrins (e.g. the Soret band of **5**, (Scheme 2) coordinated to pyridine molecules, is split to give maxima at 423 and 457 nm), and a Q-band peak at about 566 nm similar to that of five-coordinate *meso–meso*-linked zinc(II) diporphyrin **5** (Figure 5 a). These features are *entirely concentration independent* even at a very low concentrations of approximately 10^{-7} M (Figure 1), which indicates a large association constant, at least 10^{21} M^{-3}. Interestingly the fluorescence spectrum of (**Z2**)$_4$ in $CHCl_3$ clearly shows a vibrational structure ($\lambda_{max} = 613$ and 666 nm, Figure 5 b), which also differs from those of the normal *meso–meso*-linked zinc(II) diporphyins that show characteristic broader fluorescence emissions, as seen for **5** (Figure 5 b). The addition of pyridine causes the dissociation of (**Z2**)$_4$ to monomeric **Z2**, which has been monitored by the changes to the usual split Soret band ($\lambda_{max} = 423$ and 457 nm) and broader fluorescence spectrum, both of which are quite similar to those of **5** in the presence of pyridine (Figure 5). In short, the electronic interaction within

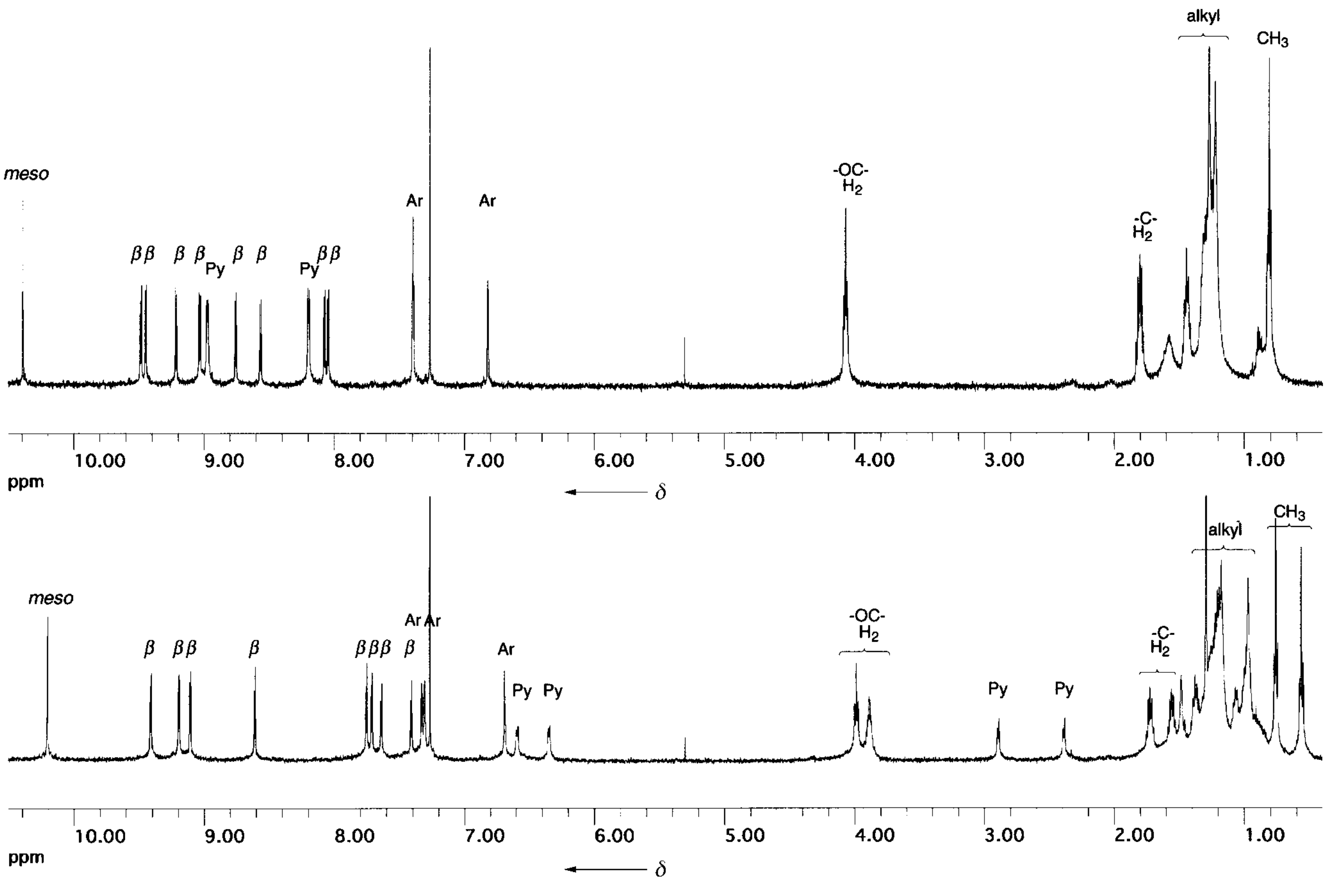

Figure 3. ^{1}H NMR spectra of **H2** (top) and (**Z2**)$_4$ (bottom) in CDCl$_3$. *meso*: porphyrin-*meso*, *β*: porphyrin-*β*, Ar: phenyl, Py: pyridyl protons.

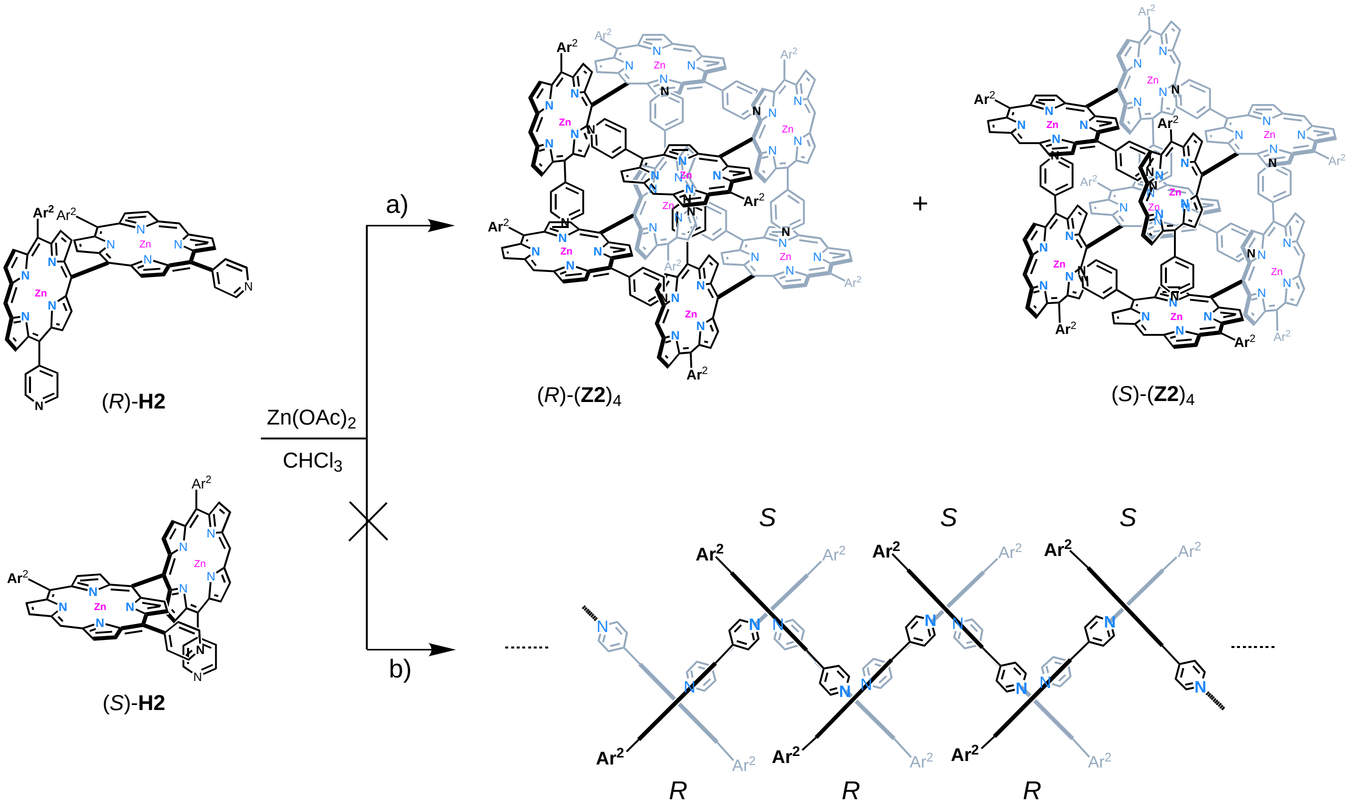

Scheme 2.

1433-7851/02/4115-2819 $ 20.00+.50/0

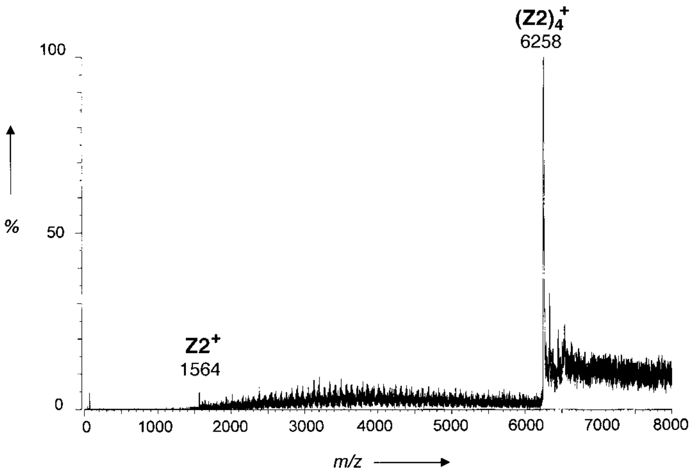

Figure 4. CSI-MS spectrum of $(\mathbf{Z2})_4$ in THF.

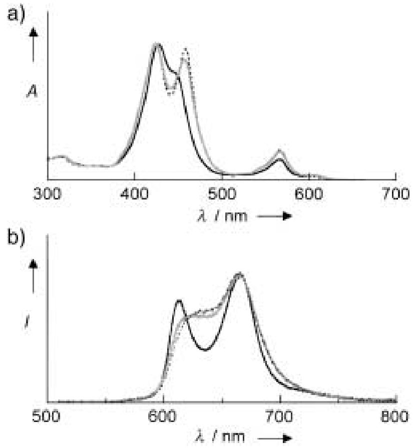

Figure 5. a) Absorption spectra of $(\mathbf{Z2})_4$ in $CHCl_3$ (——); **Z2** (from the dissociation of $(\mathbf{Z2})_4$) in $CHCl_3$ and pyridine (——); **5** in $CHCl_3$ and pyridine (----). b) Steady state fluorescence spectra of $(\mathbf{Z2})_4$ in $CHCl_3$ (——); **Z2** (from the dissociation of $(\mathbf{Z2})_4$) in $CHCl_3$ and pyridine (——); **5** in $CHCl_3$ and pyridine (----) for the excitation at 424 nm.

the *meso–meso*-linked diporphyrins is exceptionally small in $(\mathbf{Z2})_4$ in comparison to usual *meso–meso*-linked diporphyrins and is restored to the normal level upon the dissociation into monomeric **Z2**. This may be rationalized in terms of the enhanced rigidification in the $(\mathbf{Z2})_4$ assembly, where the two porphyrins in a *meso–meso*-linked diporphyrin are forced to take a rigorously perpendicular orientation, thus minimizing the electronic interaction.[14]

Given the strict perpendicular arrangement, $(\mathbf{Z2})_4$ defines a nanoscale box with a cavity of approximately $10 \times 10 \times 8$ Å. The association constant is difficult to determine but is at least $10^{25}\,\mathrm{M}^{-3}$ in $CHCl_3$ as judged from the concentration independent (up to $1.6 \times 10^{-8}\,\mathrm{M}$) fluorescence spectrum. This result indicates a remarkable degree of cooperativity in the self-assembly process, given that the each interacting motif has the same association constant. Moreover, very high stability of the aggregate $(\mathbf{Z2})_4$ has been demonstrated by its preservation even in THF,[15] in sharp contrast to **Z1**.

Owing to the different *meso*-aryl substituents, **Z2** is chiral and hence two enatiomers, (*R*)-**Z2** and (*S*)-**Z2**, are present in equal abundance in solution, since a free rotation around the *meso–meso* linkage is severely prohibited.[16] Among many possible aggregates, the sterically least demanding ones are a polymeric linear chain and a cyclic box-shaped tetramer as shown in Scheme 2. The former may be constructed by repetitive, alternate association of (*R*)-**Z2** and (*S*)-**Z2**, while the latter is formed by *self-sorting association* of (*R*)-**Z2** and (*S*)-**Z2**. The observed preferential formation of $(\mathbf{Z2})_4$ over the linear chain may be explained in terms of entropic as well as enthalpic advantages associated with a self-complementary cyclic array.

In summary, **Z1** forms a self-assembled cyclic tetramer both in solution and in the solid state only in the absence of coordinating molecules, while the *meso–meso* linked diporphyrin **Z2** forms a box-shape cyclic tetramer with an extraordinary large association constant, which is rather insensitive to coordinating molecules such as THF and alcohols. The latter aggregate compels the rigorous perpendicular orientation of the *meso–meso* linked diporphyrin, which may offer a new chance to examine the photophysical properties of the *meso–meso* linked diporphyrin with a precise perpendicular conformation.

Received: February 25, 2002
Revised: May 3, 2002 [Z18761]

---

[1] Recent reviews: a) T. Imamura, K. Fukushima, *Cood. Chem. Rev.* **2000**, *198*, 133; b) J. Wojaczynski, L. L. Grazynski, *Cood. Chem. Rev.* **2000**, *204*, 113.

[2] a) B. F. Abrahams, B. F. Hoskins, D. M. Michail, R. Robson, *Nature* **1994**, *369*, 727; b) C. M. Drain, J.-M. Lehn, *J. Chem. Soc. Chem. Commun.* **1994**, 2313; c) P. Bhyrappa, S. R. Wilson, K. S. Suslick, *J. Am. Chem. Soc.* **1997**, *119*, 8492; d) P. J. Stang, J. Fan, B. Olenyuk, *Chem. Commun.* **1997**, 1453; e) R. K. Kumar, I. Goldberg, *Angew. Chem.* **1998**, *110*, 3176; *Angew. Chem. Int. Ed.* **1998**, *37*, 3027; f) K. Kobayashi, M. Koyanagi, K. Endo, H. Masuda, Y. Aoyama, *Chem. Eur. J.* **1998**, *4*, 417; g) C. M. Drain, F. Nifiatis, A. Vasenko, J. D. Batteas, *Angew. Chem.* **1998**, *110*, 2478; *Angew. Chem. Int. Ed.* **1998**, *37*, 2344; h) S. Knapp, J. Vasudevan, T. J. Emge, B. H. Arison, J. A. Potenza, H. J. Schugar, *Angew. Chem.* **1998**, *110*, 2537; *Angew. Chem. Int. Ed.* **1998**, *37*, 2368; i) C. V. K. Sharma, G. A. Broker, J. G. Huddleston, J. W. Baldwin, R. M. Metzger, R. D. Rogers, *J. Am. Chem. Soc.* **1999**, *121*, 1137; j) C. Ikeda, N. Nagahara, E. Motegi, N. Yoshioka, H. Inoue, *Chem. Commun.* **1999**, 1759; k) D. Hagrman, P. J. Hagrman, J. Zubieta, *Angew. Chem.* **1999**, *111*, 3359; *Angew. Chem. Int. Ed.* **1999**, *38*, 3165; l) K. Ogawa, Y. Kobuke, *Angew. Chem.* **2000**, *112*, 4236; *Angew. Chem. Int. Ed.* **2000**, *39*, 4070; m) E. Iengo, B. Milani, E. Zangrando, S. Geremia, E. Alessio, *Angew. Chem.* **2000**, *112*, 1138; *Angew. Chem. Int. Ed.* **2000**, *39*, 1096; n) N. Fujita, K. Biradha, M. Fujita, S. Sakamoto, K. Yamaguchi, *Angew. Chem.* **2001**, *113*, 1768; *Angew. Chem. Int. Ed.* **2001**, *40*, 1718; o) G. A. Mines, B.-C. Tzeng, K. J. Stevenson, J. Li, J. T. Hupp, *Angew. Chem.* **2002**, *114*, 162; *Angew. Chem. Int. Ed.* **2002**, *41*, 154; p) A. Itasaka, M. Abe, T. Yoshimura, K. Tsuge, M. Suzuki, T. Imamura, Y. Sasaki, *Angew. Chem.* **2002**, *114*, 481; *Angew. Chem. Int. Ed.* **2002**, *41*, 463.

[3] a) S. Anderson, H. L. Anderson, J. K. M. Sanders, *Acc. Chem. Res.* **1993**, *26*, 469; b) J. Li, A. Ambroise, S. I. Yang, J. R. Diers, J. Seth, C. R. Wack, D. F. Bocian, D. Holten, J. S. Lindesy, *J. Am. Chem. Soc.* **1999**, *121*, 8927.

[4] M. L. Merlau, M. P. Mejia, S. T. Nguyen, J. T. Hupp, *Angew. Chem.* **2001**, *113*, 4369; *Angew. Chem. Int. Ed.* **2001**, *40*, 4239.

[5] a) S. Anderson, H. L. Anderson, A. Bashall, M. McPartlin, J. K. M. Sanders, *Angew. Chem.* **1995**, *107*, 1196; *Angew. Chem. Int. Ed.* **1995**, *34*, 1096; b) A. K. Burrell, D. L. Officer, D. C. W. Reid, K. Y. Wild, *Angew. Chem.* **1998**, *110*, 122; *Angew. Chem. Int. Ed.* **1998**, *37*, 114; c) G. S. Wilson, H. L. Anderson, *Chem. Commun.* **1999**, 1539.

[6] E. B. Fleischer, A. M. Shachter, *Inorg. Chem.* **1991**, *30*, 3763.

[7] X. Chi, A. J. Guerin, R. A. Haycock, C. A. Hunter, L. D. Sarson, *J. Chem. Soc. Chem. Commun.* **1995**, 2567.

[8] K. Funatsu, A. Kimura, T. Imamura, Y. Sasaki, *Chem. Lett.* **1995**, 765.

[9] M. Saunders, J. B. Hyne, *J. Chem. Phys.* **1958**, *29*, 1319.

[10] This crystal structure was solved based on the two zinc(II) porphyrin molecules, and the tetrameric form was obtained by its expansion. This crystal also contains fourteen disordered benzene molecules per tetraporphyrin which fill large empty spaces. Crystal data for **Z1**: $C_{78}H_{70}Zn_2N_{10}\cdot 7\,C_6H_6$, $M_r = 1825$, crystal from C_6H_6/CH_3CN, crystal dimensions $0.35\times 0.2\times 0.2$ mm, space group monoclinic ($P2_1/n$), $a = 13.7485(2)$, $b = 18.3200(3)$, $c = 40.8739(7)$ Å, $\alpha = 90$, $\beta = 84.1947(3)$, $\gamma = 90°$, $V = 10242.2(2)$ Å^3, $Z = 8$, $\rho_{calcd} = 2.367$ g cm^{-3}; $\mu_{Mo} = 10.44$ cm^{-1}; $\theta_{max} = 27.3°$. For 63126 reflections measured; $R_1 = 0.099$ for 9459 data [$I > 3\sigma(I)$], $wR_2 = 0.143$ for all measured data. The structures of all the compounds were solved by direct methods and refined by F^2 with all observed reflections. All non-hydrogen atoms without disordered *tert*-butyl group and incorporated solvent molecules were refined anisotropically, and hydrogen atoms were added to calculated positions. Programs used were structure determination by SIR92 and refinement by teXane for Windows. CCDC-173782 (**Z1**)$_4$ contains the supplementary crystallographic data for this paper. These data can be obtained free of charge via www.ccdc.cam.ac.uk/conts/retrieving.html (or from the Cambridge Crystallographic Data Centre, 12, Union Road, Cambridge CB21EZ, UK; fax: (+44)1223-336-033; or deposit@ccdc.cam.ac.uk).

[11] A. Nakano, H. Shimidzu, A. Osuka, *Tetrahedron Lett.* **1998**, *39*, 9489.

[12] a) Y. Deng, C. K. Chang, D. G. Nocera, *Angew. Chem.* **2000**, *112*, 1108; *Angew. Chem. Int. Ed.* **2000**, *39*, 1066; b) N. Aratani, A. Osuka, *Org. Lett.* **2001**, *3*, 4213.

[13] S. Sakamoto, M. Fujita, K. Kim, K. Yamaguchi, *Tetrahedron* **2000**, *56*, 955. CSI-MS spectrum measurement was performed with sector mass spectrometer (JMS-700, JEOL) equipped with the CSI source. Typical measurement conditions are as follows: (CSI-MS) acceleration voltage, 3.0 kV; needle voltage, 2.9 kV; orifice voltage, 197 V; resolution (10% valley definition), 1000; sample flow, 17 μL min^{-1}; solvent, dry THF; concentration, 10 mmol L^{-1}; spray temperature, 4 °C; ion-source temperature, 15 °C.

[14] This consideration in turn suggests that apparently stronger electronic interactions in the normal *meso–meso*-linked diporphyrins result from the rotational flexibility around the *meso–meso* single bond.

[15] Selected ^{1}H NMR signals of the pyridyl groups of (**Z2**)$_4$ in [D$_8$]THF; $\delta = 2.62$, 3.11, 6.59, and 6.86 ppm.

[16] N. Yoshida, A. Osuka, *Tetrahedron Lett.* **2000**, *41*, 9287.

Crystal Engineering of a Nanoscale Kagomé Lattice[**]

Brian Moulton, Jianjiang Lu, Ranko Hajndl,
Srikanth Hariharan, and Michael J. Zaworotko[*]

What would the properties of materials be if we could really arrange the atoms the way we want them? Although this question is scientifically and technologically topical, it is a well-known excerpt from the Richard P. Feynman lecture "There's Plenty of Room at the Bottom".[1] Recent advances in our understanding of supramolecular chemistry offer promise that Feynman's dream will be realized since they have afforded design principles that have provided access to an array of new solid phases with specific and, in many cases, previously unknown molecular topologies. Indeed, as molecular scientists become ever more proficient at the supramolecular synthesis[2] of new compositions and structures, the question that might now be posed is: "in what manner do we want to arrange the atoms?" In the context of magnetic materials, theorists have provided chemists with an array of target lattices,[3] and synthetic chemists have developed new strategies for the generation of novel networks that contain magnetic components.[4–7] Spin-frustrated lattices represent attractive targets that are exemplified by the antiferromagnetic Kagomé lattice.[8] Herein we present the synthesis, crystal structure, and magnetic properties of, what is to our knowledge, the first example of a nanoscale Kagomé lattice.

The phase is sustained by paramagnetic dicopper(II) tetracarboxylate spin pairs (metal dimers) positioned at the vertices of a Kagomé lattice, and it exploits the concept of self-assembly of nanoscale secondary building units (nSBUs).[9] It therefore offers a system where the effect of systematically substituting the molecular components can be evaluated. In this context, we compare the magnetic response of the Kagomé lattice arrangement with a system where identical secondary building units (SBUs)[10] are arranged in a tetragonal 2D configuration, which is not expected to exhibit spin frustration.

We have recently demonstrated that regular molecular squares can self-assemble at their vertices to form square or triangular nSBUs, and that the use of an appropriate template and mild crystallization conditions facilitates the generation of a diverse range of discrete and infinite molecular architectures that are based upon these nSBUs.[9, 11–13] The ubiquitous dimetal tetracarboxylates $[M_2L_2(O_2CR)_4]$ (L = coordinated ligand, M = transition metal) serve as ideal molecular squares in this context since they are synthetically accessible and, depending upon the metal, offer potential as catalysts[14] or molecular magnets.[15, 16] Figure 1 illustrates the two nSBUs that can be generated if the molecular squares are linked by 1,3-benzenedicarboxylate (bdc), that is, at 120°: a square nSBU (a cluster of four square SBUs) or a triangular nSBU (a cluster of three square SBUs). These nSBUs are known to self-assemble to form discrete nanoballs (sustained by both square and triangular nSBUs)[12] or a tetragonal 2D lattice (sustained by square nSBUs only).[9] It occurred to us that other supramolecular isomers are possible if triangular nSBUs alone are present: triangular or Kagomé 2D lattices (Figure 2). Few examples of molecular Kagomé lattices have been reported to date,[17–19] and to our knowledge there have been no reports of a nanoscale lattice, despite the expectation of cooperative magnetic phenomena in such structures.

Slow diffusion of ethanolic copper(II) nitrate into a solution of bdc, pyridine (py), and an appropriate template (nitrobenzene, 1,2-dichlorobenzene, or naphthalene) in ethanol affords prismatic blue-green crystals of $[(Cu_2(py)_2(bdc)_2)_3]_n$ (**1**). The crystal structure of **1**[20] (Figure 3) can be described as

---

[*] Prof. Dr. M. J. Zaworotko, B. Moulton, J. Lu
Department of Chemistry
University of South Florida
4202 E. Fowler Ave., SCA 400, Tampa, FL 33620 (USA)
Fax: (+1) 813-974-1733
E-mail: xtal@usf.edu

R. Hajndl, Prof. Dr. S. Hariharan
Department of Physics
University of South Florida
4202 E. Fowler Ave., PHY 114, Tampa, FL 33620 (USA)

[**] M.J.Z. gratefully acknowledges the financial support of the National Science Foundation (DMR-0101641). S.H. acknowledges support from a DARPA/AMRI subcontract (Grant No. MDA 972-97-1-0003).

1433-7851/02/4115-2821 $ 20.00+.50/0